254. Crystal Structure and Electrical Conductivity of Nickel 6,13-Di(*p*-tolyl)-5,14-dihydrodibenzo[*b*, *i*]-1,4,8,11-tetraaza[14]annulene Iodide (Ni(dtdbtaa)$I_{2.58}$)

by **Max Hunziker, Hans Loeliger, Grety Rihs** and **Bruno Hilti**

Zentrale Forschungslaboratorien, *Ciba-Geigy AG*, CH-4002 Basel

(17.IX.81)

Summary

Single crystals of the title compound are monoclinic, space group $P2_1/n$ with two formula units per cell of the following dimensions: $a = 18.209$, $b = 19.076$, $c = 4.075$ Å, $\beta = 92.43°$. The crystals show metallic conductivity along the needle axis from room temperature down to *ca.* 180 K, the maximum conductivity at room temperature being 455 $(\Omega\,\mathrm{cm})^{-1}$.

The unoxidized (iodine free) parent compound crystallizes in the monoclinic space group $P2_1/c$ with 2 molecules per cell of dimensions: $a = 4.988$, $b = 20.192$, $c = 11.871$ Å, $\beta = 94.41°$.

1. Introduction. – It has recently been shown [1–3] that partial oxidation of metallotetraaza[14]annulenes by iodine leads to a large new class of highly conductive materials in which the properties can be manipulated by variation of the substituents and/or the central metal ion. In order to understand the effect of various substituents and metal atoms on the conductivity (and other physical properties) it is essential to obtain the data of single crystals of appropriate size and quality. Due to the difficulties experienced in growing crystals, most data published today refer to powders [1–3], often with various degrees of oxidation, *i.e.* iodine content. Only rarely have single crystals been obtained [1] [2] and examples where crystals grew to dimensions suitable for X-ray work are even more scarce. The structures of only two isomorphous iodides, Ni(dbtaa)I_2 and Pd(dbtaa)I_2 (dbtaa = dibenzo[*b*, *i*]-1,4,8,11-tetraaza[14]annulene), are currently known [2].

Here we demonstrate the effect of the relatively bulky tolyl substituents in the meso-positions of nickeldibenzo[*b*, *i*]-1,4,8,11-tetraaza[14]annulene on the structure and conductivity of the neutral and partially oxidized product.

2. Experimental. – *Preparation of Ni(dtdbtaa).* This complex was prepared by refluxing Ni(pd)$_2$Cl$_2$ (pd = *o*-phenylenediamine) [4] and 2-(*p*-tolyl)malondialdehyde [5] in DMF for 16 h. The raw product was purified by multiple sublimation *in vacuo* at 10^{-3} Torr and 300°. Single crystals of the pure macrocycle suitable for X-ray analysis were grown in DMF solutions. Single crystals of Ni(dtdbtaa)$I_{2.58}$ were prepared by codiffusion of (Ni(dtdbtaa)) and iodine in 2:1 mixtures of doubly distilled 1,2,4-trichlorobenzene and dichloromethane, using a modified type of H-tube. No other stoichiometries were found by varying the iodine concentration over a wide range.

0018-019X/81/8/2544-11$01.00/0

Table 1. *Crystal data and refinement of Ni(dtdbtaa) and Ni(dtdbtaa)$I_{2.58}$*

Compound	$Ni(C_{32}H_{26}N_4)$	$Ni(C_{32}H_{26}N_4)I_{2.58}$
Molecular weight	525.3	852.7
Cell: a [Å]	4.988	18.209
b [Å]	20.192	19.076
c [Å]	11.871	4.075
β [°]	94.41	92.43
V [Å^3]	1192	1414
Z	2	2
Density, g/cm^3 calc.	1.463	2.002
found	1.461	1.988
Space group	$P2_1/c$	$P2_1/n$
Radiation	Mo$K\alpha$	Mo$K\alpha$
Unique data with $I \geq 2\sigma$ (I)	1500	2194
Final R-factor	0.037	0.083
Final number of parameters	221	241

X-Ray analysis of Ni(dtdbtaa). A fragment with dimensions $0.5 \times 0.12 \times 0.04$ mm^3 was cut from a larger column. Crystals are monoclinic, space group $P2_1/c$ (centrosymmetric). Crystal data presented in *Table 1* were obtained by the usual procedures on a *Philips PW 1100* diffractometer using MoK_α radiation. Calculated and experimental densities compare favorably. The structure was solved by direct methods (MULTAN 77). Block-diagonal least-squares refinements with anisotropic temperature

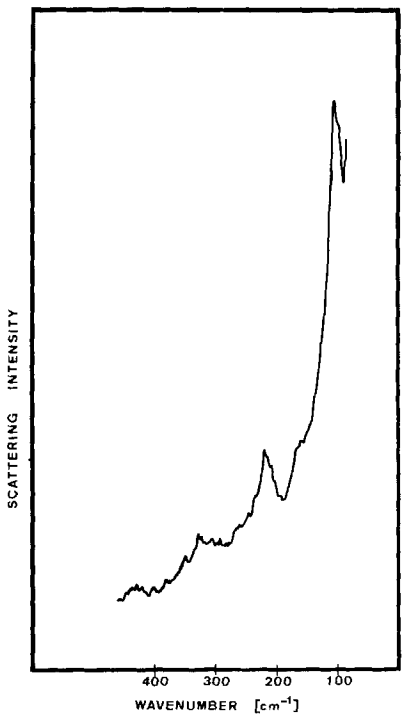

Fig. 1. *Resonance*-Raman *spectrum of a solid sample of Ni(dtdbtaa)$I_{2.58}$* (spinning KBr disc, $v_0 = 4880$ Å; I_3^--symmetric stretching fundamental at 106 cm^{-1} and overtone progression)

factors for the 19 non-H-atoms converged at R = 0.058. All 13 H-atoms could be located in a difference *Fourier* synthesis. With all atoms included, R dropped to a final value of 0.037.

X-Ray analysis of Ni(dtdbtaa)$I_{2.58}$. Owing to the fragile nature of the crystals, cutting to the desired length was impossible. The needle-shaped crystals had to be used as they were. A crystal of dimensions $2 \times 0.15 \times 0.07$ mm^3 was used for the analysis. Crystals are again monoclinic, space group $P2_1/n$.

Cell constants *(Table 1)* were obtained as above. *Weissenberg* photographs showed diffuse lines parallel to the plane a^*b^* in addition to the normal *Bragg* scattering from the lattice of the nickel macrocycle. The diffuse lines are attributed to a disordered incommensurate sublattice of I-atoms. The intensity distribution of the diffuse lines is very similar to that found for the iodine sublattice in TTT_2I_3 [6]. The periodicity of the superstructure of 9.48 Å indicates that iodine might be present as I_3^--ions. This was confirmed by resonance-*Raman* scattering [7] *(Fig. 1)*. The structure was solved by the classical heavy-atom method. As the unit cell contains only two nickel macrocycles the molecule must have C_i-symmetry. From a 3-dimensional *Patterson* synthesis the positions of the nickel and the iodine atoms were obtained. Structure factor calculations and *Fourier* syntheses then led to the localization of all non-H-atoms. Additional electron density was observed from the disordered iodine arrangement. A number of different models for this were tested. Best results were achieved with a model consisting of 8 I-atoms distributed uniformly along the c-direction with the sum of occupancies equalling 1.29. Block-diagonal least-squares refinement with anisotropic temperature factors converged at R = 0.083 for all *hkl* reflections. The H-atoms could not be located. In the *hk*0 projection the parameters could be refined to an R factor of 0.042 with a ratio of nickel macrocycle to iodine of 1:2.58. This value was obtained by comparison of the c-periodicities of the two sublattices. We analyzed four crystals and consistently found a ratio of $1:2.56 \pm 0.02$. This value agrees with the ratio obtained from elemental analysis of 1:2.6 and is further confirmed by the measured density *(Table 1)*.

Table 2. *Bond lengths and bond angles* (Å and deg respectively)

Atoms	$Ni(C_{32}H_{24}N_4)$	$Ni(C_{32}H_{24}N_4)I_{2.56}$	Atoms	$Ni(C_{32}H_{24}N_4)$	$Ni(C_{32}H_{24}N_4)I_{2.56}$
Ni–N(2)	1.860 (3)	1.868 (8)	C(4)–C(3)–N(2)	126.1 (4)	126.3 (9)
Ni–N(9)	1.851 (3)	1.871 (8)	C(8)–C(3)–N(2)	113.6 (3)	114.1 (9)
N(2)–C(3)	1.412 (5)	1.401 (13)	C(3)–C(4)–C(5)	119.1 (4)	119.8 (9)
C(3)–C(4)	1.388 (6)	1.442 (14)	C(4)–C(5)–C(6)	120.6 (4)	122.6 (13)
C(3)–C(8)	1.393 (6)	1.400 (14)	C(7)–C(6)–C(5)	120.7 (4)	115.1 (16)
C(4)–C(5)	1.389 (6)	1.415 (15)	C(6)–C(7)–C(8)	118.3 (4)	123.1 (12)
C(5)–C(6)	1.393 (7)	1.424 (21)	C(3)–C(8)–C(7)	120.9 (4)	119.5 (9)
C(6)–C(7)	1.393 (6)	1.453 (21)	C(3)–C(8)–N(9)	113.5 (3)	116.3 (9)
C(7)–C(8)	1.398 (6)	1.413 (14)	C(7)–C(8)–N(9)	125.6 (4)	124.1 (9)
C(8)–N(9)	1.421 (5)	1.392 (13)	C(10)–N(9)–C(8)	119.3 (3)	120.8 (9)
N(9)–C(10)	1.330 (5)	1.313 (13)	C(10)–N(9)–Ni	127.0 (3)	128.6 (7)
C(10)–C(11)	1.405 (6)	1.394 (15)	C(8)–N(9)–Ni	113.6 (2)	110.5 (6)
C(11)–C(12)	1.393 (6)	1.377 (16)	N(9)–C(10)–C(11)	124.3 (4)	124.2 (10)
C(11)–C(13)	1.484 (6)	1.508 (14)	C(12)–C(11)–C(10)	122.6 (4)	122.1 (9)
C(13)–C(14)	1.403 (6)	1.381 (17)	C(12)–C(11)–C(13)	119.3 (4)	119.2 (9)
C(13)–C(18)	1.414 (6)	1.391 (15)	C(10)–C(11)–C(13)	118.0 (4)	118.7 (10)
C(14)–C(15)	1.392 (6)	1.382 (14)	N(2)–C(12)–C(11)	124.3 (4)	125.4 (10)
C(15)–C(16)	1.394 (6)	1.395 (16)	C(14)–C(13)–C(18)	116.5 (4)	123.2 (9)
C(16)–C(17)	1.378 (6)	1.398 (15)	C(14)–C(13)–C(11)	122.2 (4)	118.7 (9)
C(16)–C(19)	1.520 (7)	1.529 (15)	C(18)–C(13)–C(11)	121.3 (4)	118.1 (9)
C(17)–C(18)	1.407 (6)	1.409 (15)	C(15)–C(14)–C(13)	121.7 (4)	118.2 (11)
N(9)–Ni–N(2)	85.7 (1)	87.7 (3)	C(14)–C(15)–C(16)	120.9 (4)	121.4 (11)
N(9)–Ni–N(2′)	94.3 (1)	92.3 (3)	C(17)–C(16)–C(15)	119.0 (4)	118.9 (10)
C(12)–N(2)–C(3)	119.4 (4)	121.4 (9)	C(17)–C(16)–C(19)	120.8 (4)	122.3 (10)
C(12)–N(2)–Ni	127.0 (2)	127.2 (6)	C(15)–C(16)–C(19)	120.2 (4)	118.6 (10)
C(3)–N(2)–Ni	113.6 (2)	111.4 (6)	C(16)–C(17)–C(18)	120.5 (4)	120.9 (10)
C(4)–C(3)–C(8)	120.3 (4)	119.6 (9)	C(17)–C(18)–C(13)	121.4 (4)	117.0 (9)

ESR. spectroscopy. ESR. spectroscopy was performed on samples of Ni(dtdbtaa)$I_{2.58}$ between 97 and 295 K. Batches of single crystals (20–40) with lengths between 2.5 and 6 mm and a total weight of 0.4–0.8 mg were aligned in a quartz-capillary of 1 mm diameter. For the *g*-anisotropy measurements a special teflon holder allowing angle variation from $H_0 \parallel c$, $H_1 \perp c$ to $H_0 \perp c$, $H_1 \perp c$ was used. No ferromagnetic impurities were found.

Electrical conductivity measurements. The electrical conductivity of Ni(dtdbtaa)$I_{2.58}$ single crystals was determined along the needle axis (c) by a conventional four-probe DC. technique using gold wires as supporting electrodes and Pt-paste as contacts. The temperature dependence of the conductivity was determined by cooling the crystals at a rate of approx. 0.3°/min.

3. Results and discussion. – *Description of the structures.* Bond lengths and angles are given in *Table 2* for both Ni(dtdbtaa) and Ni(dtdbtaa)$I_{2.58}$. The atom-labeling scheme is shown in *Figure 2. Figure 3* is a projection of the Ni(dtdbtaa)

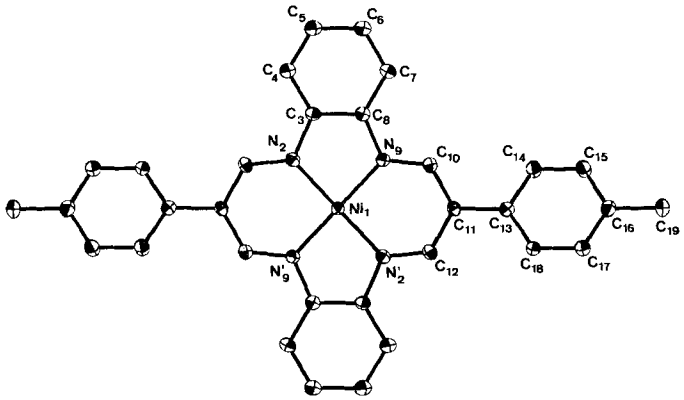

Fig. 2. *Atom-labeling scheme for the macrocyclic molecule* (elipsoids for all drawings are at 20% probability)

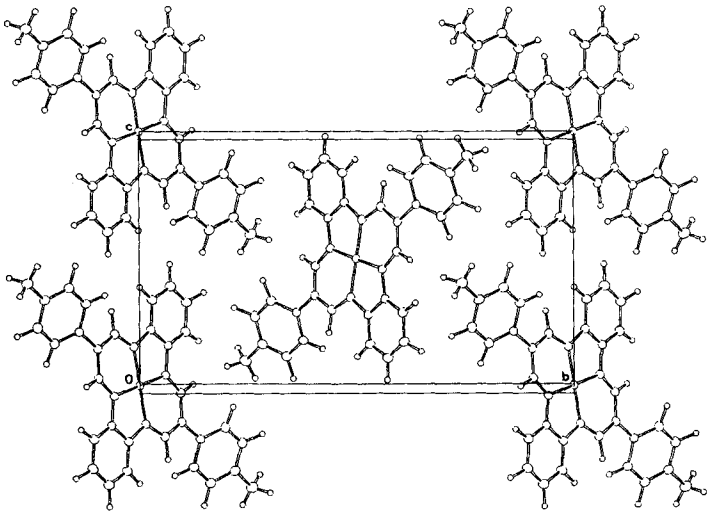

Fig. 3. *Projection of the Ni(dtdbtaa) structure on the* b,c-*plane*

structure on the *b, c*-plane. The molecules are stacked along [100] (needle axis) with an intermolecular distance of 3.38 Å. *Figure 4* illustrates the packing in projection on the *a, b*-plane. A similar packing pattern is usually observed for large planar aromatic molecules and was also found for the unsubstituted macrocycle Ni(dbtaa) [8] and a variety of substituted derivatives [9]. The overlap of two adjacent molecules within a stack is shown in *Figure 5*. The Ni, Ni-distance of 4.988 Å corresponds to the *a*-periodicity.

The benzene ring of the tolyl substituent does not lie in the same plane as the tetraazaannulene but is rotated around the axis C_{11}–C_{13} by 22°. This deviation from planarity is caused by steric repulsion between the H-atoms on C_{10}, C_{14} and C_{12}, C_{18}. While the *van der Waals* diameter of hydrogen is 2.4 Å [10], the observed distances between H-atoms on C_{10}, C_{14} and C_{12}, C_{18} are 2.11 and 2.14 Å, respectively.

Except for the Ni-N_4 coordination unit, the dibenzotetraaza[14]annulene system itself is not strictly planar, C-atoms in the benzenoid ring deviating by up to 0.18 Å from this plane (see *Table 3*). The average C, C-bond length in the benzo ring is 1.392 Å, that in the tolyl substituent is 1.398 Å. Both values are close to the standard value of 1.394 Å [11].

In the structure of Ni(dtdbtaa)$I_{2.58}$ the type of packing is essentially the same, with chains of iodine atoms confined to the channels between the stacks of the macrocycles. *Figure 6* shows a projection of the structure on the *a, b*-plane and illustrates the location of the iodine chains. *Figure 7* shows the tilt of the macrocycle to the stacking axis. The Ni, Ni-distance of 4.075 Å corresponds to the *c*-periodicity. Although this is shorter than in Ni(dtdbtaa), the overlap diagram *(Fig. 8)* makes it clear that no strong Ni, Ni-interaction can be expected. The intermolecular separation, however, is reduced by oxidation from 3.38 to 3.23 Å, a value in line with other examples of highly conducting metallomacrocycles [2] [12]. The particular structural arrangement found here makes it evident that the high electrical conductivity in the oxidized compound is caused by the overlap of partially filled ligand π-orbitals. That oxidation is ligand-centered is clearly manifested in the bond lengths (as well as by the *g*-values) *(vide infra, Table 2)*. While in the unoxi-

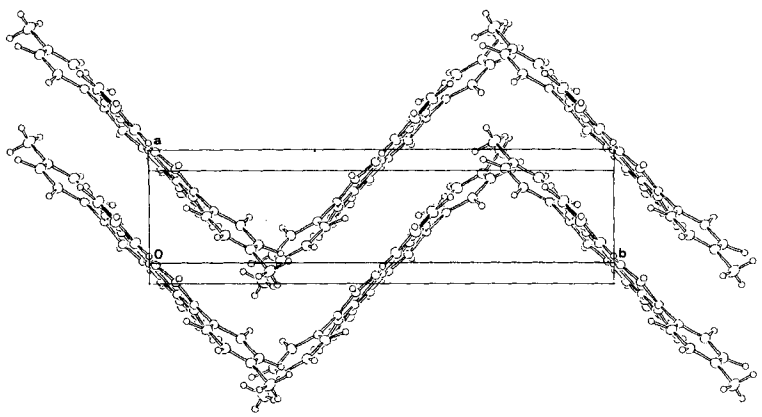

Fig. 4. *Projection of the Ni(dtdbtaa) structure on the* a, b-*plane*

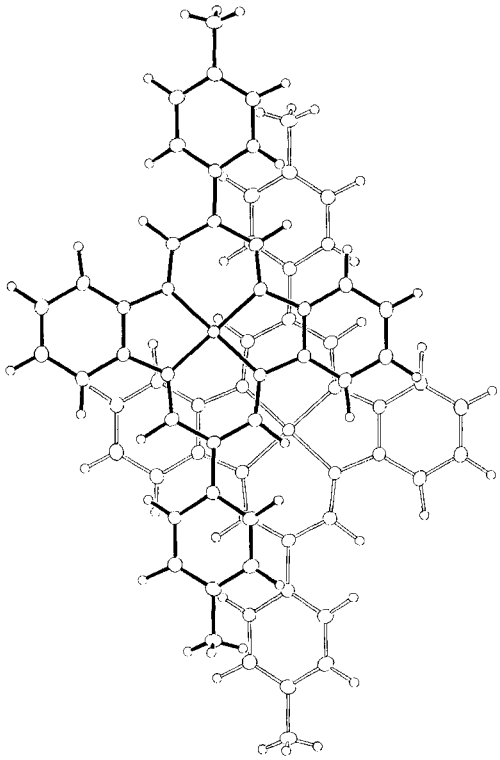

Fig. 5. *Overlap of two adjacent molecules in Ni(dtdbtaa) crystals*

dized macrocycle the average C,C-bond length in the benzo ring is 1.392 Å, on oxidation it becomes 1.425 Å. The increase of 0.033 Å can be explained by a decrease in π-electron density, *i.e.* bond order. The same effect had already been observed in the case of Ni(dbtaa)I_2 [2] but is more pronounced in the present example. Average C,C-bond lengths in the tolyl substituent remain essentially unchanged (1.398 and 1.393 Å for the neutral and the oxidized molecules, respectively). In the heterocyclic six-membered ring $Ni_1, N_9, C_{10} \ldots N_2'$ (see *Fig. 2*) the average of the two C,C-bond lengths is slightly shorter (0.013 Å) in the oxidized macrocycle, contrasting with Ni(dbtaa)I_2 where these bonds were lengthened by about 0.02 Å. The tetraazaannulene moiety is more closely planar in the oxidized

Table 3. *Deviations from the plane through the N-atoms* [Å]

Atom	$Ni(C_{32}H_{24}N_4)$	$Ni(C_{32}H_{24}N_4)I_{2.58}$	Atom	$Ni(C_{32}H_{24}N_4)$	$Ni(C_{32}H_{24}N_4)I_{2.58}$
Ni	0	0	C(7)	−0.16	−0.09
N(2)	0	0	C(8)	−0.04	−0.02
C(3)	0.00	−0.01	N(9)	0	0
C(4)	−0.02	−0.02	C(10)	0.09	−0.02
C(5)	−0.10	−0.07	C(11)	0.05	−0.06
C(6)	−0.18	−0.04	C(12)	−0.04	0.00

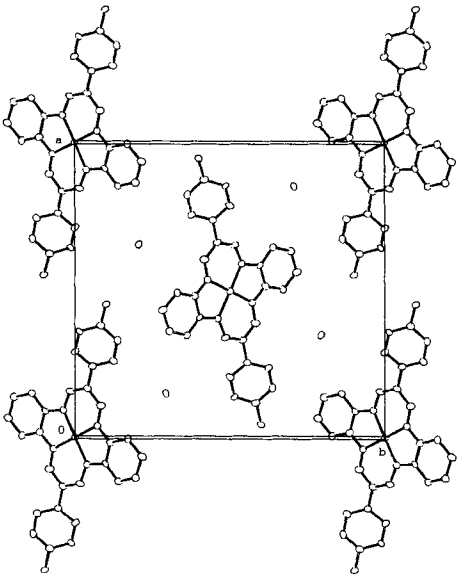

Fig. 6. *Projection of the* $Ni(dtdbtaa)I_{2.58}$ *structure on the* a,b-*plane*

complex *(Table 3)*. This may be due to the tighter packing of the molecules and to the fact that the tolyl substituents are rotated more (by 31°) out of the tetraaza-annulene plane, thus eliminating most of the steric repulsion between interacting H-atoms.

ESR. results. – g-*Values.* Single crystals of $Ni(dtdbtaa)I_{2.58}$ show a single, rather broad ESR. signal of moderate intensity. Characteristic ESR. data for two samples are compiled in *Table 4*. Around room temperature the large line width (160–180 G) complicates the determination of the *g*-values. Even at lower temperatures (97 K) the line width is more than 20 times larger than in $NiPcI_{1.0}$ (= nickel phthalocyanine iodide) [12] or $Ni(OMTBP)I_{1.08}$ (= nickel octamethyltetrabenzoporphinato iodide) [13]. Within experimental error, the *g*-values and *g*-anisotropy remain constant over the temperature range of 97 to 300 K. Since the *g*-anisotropy is relatively

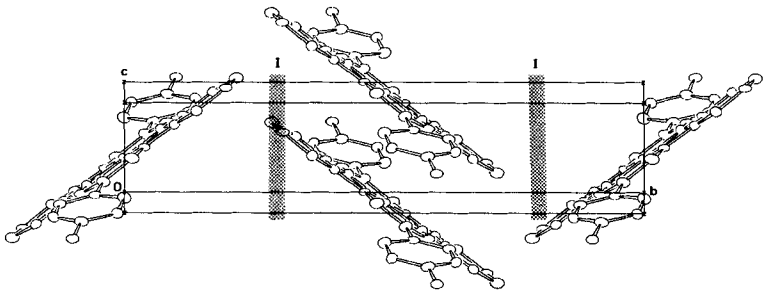

Fig. 7. *Stacking of the macrocyclic molecules in* $Ni(dtdbtaa)I_{2.58}$ *illustrated in a projection on the* b,c-*plane*

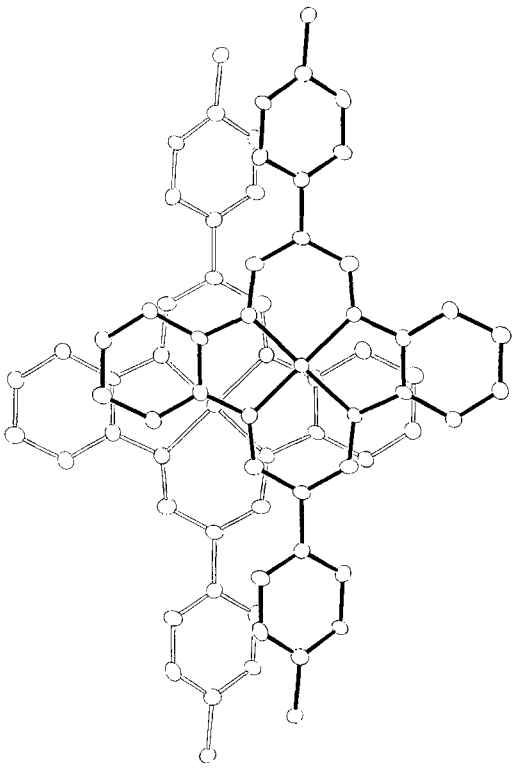

Fig. 8. *Overlap of two neighbouring molecules of a stack in Ni(dtdbtaa)$I_{2.58}$*

small *(Table 4)* we did not determine the exact angular dependence of g. Both $g_\parallel$ and $g_\perp$ are very close to and slightly less than the free electron value, $g_e = 2.0023$. This confirms that the oxidation is ligand-centered, since metal-centered oxidation would yield a Ni(III)-species with a g-value far from g_e and anisotropies (defined by $\Delta g \equiv |g_\parallel - g_\perp|$) about 50 to 100 times larger than in the present case where Δg amounts to only 0.0016.

This is in line with ESR. results on Ni(dbtaa)$I_{2.0}$ where we also observed g-values near g_e and very small g-anisotropies, again consistent with ligand-centered oxidation. In $[Ni(III)Pc]^+$, where Ni(III) lies in a coordination environment comparable to our examples, g-values of 2.29 ($g_\perp$) and 2.11 ($g_\parallel$) have been

Table 4. *Characteristic ESR. data for Ni(dtdbtaa)$I_{2.58}$*

Sample	T [K]	X^s_M 10^{-6} [cm^3/mol]	Spins per macrocycle	Line width ΔHpp [G]	$g\perp$ ($H_0 \perp c$; $H_1 \parallel c$; $H_1 \perp c$)	$g_\parallel$ ($H_0 \parallel c$; $H_1 \perp c$)	$\bar{g}$
1	283	140	0.11 (4)	180	2.0019 (5)		
1	97	80	0.065 (25)	25	2.0018 (1)	2.00025 (5)	2.00128 (10)
2	295	140	0.11 (4)	162	2.0019 (3)		
2	97	40	0.03 (1)	26	2.0019 (3)		

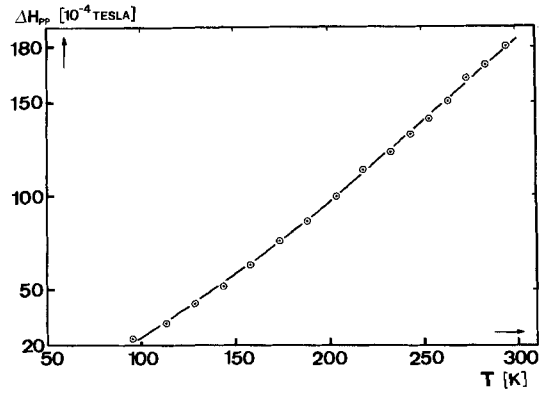

Fig. 9. *Temperature-dependence of the ESR. line-width for Ni(dtdbtaa)$I_{2.58}$ crystals*

determined [14]. Thus, together with the X-ray and resonance-*Raman* results, Ni(dtdbtaa)$I_{2.58}$ may be formulated as Ni(II) $(dtdbtaa)^{0.86+}(I_3^-)_{0.86}$.

Line width. The ESR. signal is Lorentzian throughout the temperature range from 97 to 300 K for all orientations of the crystals relative to H_0 and H_1. The line width shows no angular dependence but it is temperature dependent, becoming narrower with decreasing temperature *(Fig. 9)* with perhaps a slight change of slope in the region of the conductivity maximum (around 180 K).

ESR. intensity. The absolute ESR. intensity measurements at room temperature show 0.11 (4) spins per macrocycle *(Table 4)*, a value comparable to that of 0.14 found for $NiPcI_{1.0}$ [12]. Below room temperature the ESR. intensity drops off smoothly *(Fig. 10)* with minor irregularities around the conductivity maximum at 180 K and possibly elsewhere as well. No static susceptibility measurements could be made, owing to the small amount of crystalline material available.

Single crystal conductivity of Ni(dtdbtaa)$I_{2.58}$. The electrical conductivity was measured only along the needle axis, the crystals being too thin to determine transverse conductivities. Room temperature conductivities lie around 100 $(\Omega\,\mathrm{cm})^{-1}$

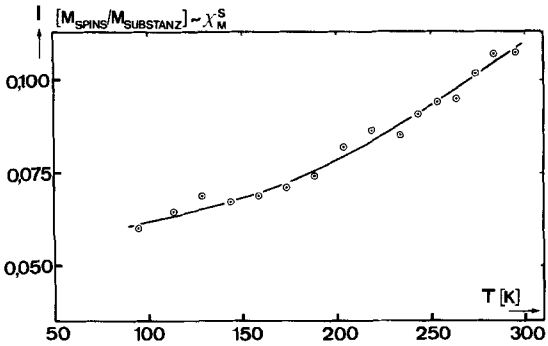

Fig. 10. *Temperature-dependence of the ESR.-signal intensity* (proportional to the molar spin susceptibility χ_m^S) *in number of free spin per macrocycle for crystals of Ni(dtdbtaa)$I_{2.58}$*

with a maximum value of 455 $(\Omega\,\mathrm{cm})^{-1}$. These values are comparable to conductivities of other partially oxidized metallomacrocycles [2] [12] and organic metals such as TTF-TCNQ [15].

The mean free path, λ, of a charge carrier (along the stacking direction) ranges from 1 to 4.5 Å or 0.3 to 1.4 lattice spacings. This is only about half of that found for $NiPcI_{1.0}$ and Ni(tetrabenzporphyrin)$I_{1.0}$ [12] [13b] and is indicative of transport properties in the borderline region between diffusive and coherent conductivity.

The temperature dependence of the conductivity is metallic down to *ca.* 180 K where the substance transforms to quasi semi-conducting behaviour *(Fig. 11)*. Below 120 K the conductivity can be fitted to an *Arrhenius*-type plot (least squares fit to $\sigma = \sigma_0 \exp[-Ea/2kT]$) with a constant activation energy of 0.064 (6) eV.

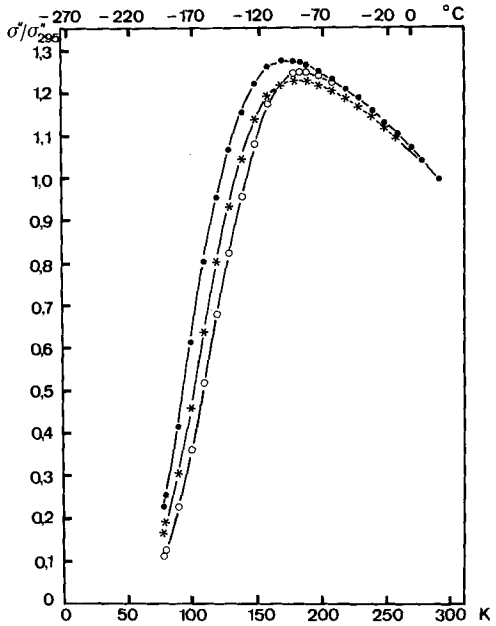

Fig. 11. *Temperature-dependence of the conductivity ratio* $\sigma_{\parallel}(T)/\sigma_{\parallel}$ (295 K) *for three Ni(dtdbtaa)*$I_{2.58}$ *crystals of the following room-temperature conductivities:* * = 64, ● = 112 and ○ = 455 $(\Omega\,\mathrm{cm})^{-1}$

4. Conclusion. – Many square-planar transition-metal complexes with macrocyclic or other organic ligands are known to crystallize in slipped stack structures, *i.e.* molecular plane not perpendicular to the stacking axis [8] [16]. However, on partial oxidation, the structures of all currently known highly conducting metal complexes are changed to a stacking pattern where the molecular planes are perpendicular to the stacking direction, resulting in relatively short metal-metal distances with the possibility of interaction. Indeed, *Endres et al.* [16] have suggested that high electrical conductivity is restricted to this latter type of structure. This may hold as long as the metal atom is involved in the oxidation process. If, however, oxidation is ligand-centered (as in our example), conductivity may occur

because of overlap of ligand π-orbitals, thus making the stacking angle unimportant. To the best of our knowledge, Ni(dtdbtaa)$I_{2.58}$ is the only highly conducting transition-metal complex with a slipped stack arrangement. Obviously, the two meso-positioned tolyl substituents are responsible for this unique structural arrangement; the parent compound Ni(dbtaa)$I_{2.0}$ (without substituents) has a perpendicular stacking [2].

The authors wish to thank *H.R. Walter* and *J. Pfeiffer* for experimental assistance and *S. Moss* for the resonance-*Raman* spectrum.

REFERENCES

[1] a) *L. Lin, T.J. Marks, C.R. Kannewurf, J.W. Lyding, M.S. McClure, M.T. Ratajack & T.-C. Whang,* J. Chem. Soc., Chem. Commun. *1980*, 954; b) *M.S. McClure, L.-S. Lin, T.-C. Whang, M.T. Ratajack, C.R. Kannewurf & T.J. Marks,* Bull. Am. Phys. Soc. *25*, 315 (1980); c) *W.E. Hatfield,* U.S. Gov. Rep. TR-10, AD-AO83765 and TR-12, AD-AO89940 (1980).
[2] *M. Hunziker, B. Hilti & C. Rihs,* Helv. Chim. Acta *64*, 82 (1981).
[3] *Y.-M. Wuu, S.-M. Peng & H. Chang,* J. Inorg. Nucl. Chem. *42*, 839 (1980).
[4] *W. Hieber, C. Schliessmann & K. Ries,* Z. Anorg. Allg. Chem. *180*, 89 (1929).
[5] *G.M. Coppala, G.E. Hardtman & B.S. Huegi,* J. Heterocycl. Chem. *11*, 51 (1974).
[6] *D.L. Smith & H.R. Luss,* Acta Crystallogr. *B33*, 1744 (1977).
[7] *T.J. Marks, D.F. Webster, S.L. Ruby & S. Schultz,* J. Chem. Soc., Chem. Commun. *1976*, 444.
[8] *M.C. Weiss, G. Gordon & V.L. Goedken,* Inorg. Chem. *16* (2), 305 (1977).
[9] *M. Hunziker & G. Rihs,* unpublished results.
[10] *L. Pauling,* 'The Nature of the Chemical Bond', Cornell University Press 1960.
[11] Interatomic distances, Special publication No. 18, The Chemical Society, London 1965.
[12] *C.J. Schramm, R.P. Scaringe, D.R. Stojakovič, B.M. Hoffman, J.A. Ibers & T.J. Marks,* J. Am. Chem. Soc. *102*, 6702 (1980).
[13] a) *T.E. Phillips, R.P. Scaringe, B.M. Hoffman & J.A. Ibers,* J. Am. Chem. Soc. *102*, 3435 (1980); b) *B.M. Hoffman et al.,* in 'Molecular Metals', edited by W.E. Hatfield, Plenum Press New York, London 1979.
[14] *A.P. Bobrovskii & A.N. Sidorov,* J. Struct. Chem. (Engl. Transl.) *17*, 50 (1976).
[15] *J.B. Torrance,* Acc. Chem. Res. *12*, 79 (1979).
[16] *H. Endres, H.J. Keller, R. Lehmann, A. Poveda, H.H. Rupp & H. van de Sand,* Z. Naturforsch. *32b*, 516 (1977) and references cited therein.